

**E-SKIN RESISTIVE STRAIN SENSOR: OPTIMUM SENSOR PLACEMENT**

**A Technical Report submitted to the Department of Mechanical Engineering**

**Presented to the Faculty of the School of Engineering and Applied Science**

**University of Virginia • Charlottesville, Virginia**

**In Partial Fulfillment of the Requirements for the Degree**

**Bachelor of Science, School of Engineering**

**Zachary Holden**

**Spring, 2022**

**Technical Project Team Members**

**Denis Chavarria**

**Sohail Ghatnekar**

**Nick Johnson**

**On my honor as a University Student, I have neither given nor received unauthorized aid  
on this assignment as defined by the Honor Guidelines for Thesis-Related Assignments**

**Baoxing Xu, Department of Mechanical Engineering**

## ABSTRACT

This project serves as an application of the cutting-edge work that has been done with transparent, elastic conductors, which are paving the way for the development of wearable devices with the ability to conform to the curved, irregular surfaces of the human body (Ray et al., 2019). E-skin sensors will be the future of wearable exercise technology, and this minimally invasive device will be a step in the direction of fully functioning continuous tracking technology. The sensor, designed in Solidworks, is a body-conforming resistive strain and temperature sensor that fits onto the anterior deltoid. While the sensor was unable to be tested on human subjects due to time and monetary restraints, it was designed, manufactured, fabricated, and tested in a mechanical setting for its temperature measuring capabilities. This report details the design considerations, and manufacture, fabrication and testing of the sensors. The sensor, made of polydimethylsiloxane (PDMS) and multi-walled carbon nanotubes (MWCNTs), was tested for the repeatability and the resistance to temperature relationship, by calculating the coefficient of temperature. The coefficient of temperature was very similar for both sensors analyzed, and indicates that the device and process could be repeated for further testing in the future. Further applications and future research could include further testing of various device iterations, as well as mechanical strain testing.

## TABLE OF CONTENTS

<b>INTRODUCTION</b> .....	p. 1
<b>DESIGN THEORY AND WORKING PRINCIPLE</b> .....	p. 1
<b>DESIGN AND FABRICATION</b> .....	p. 6
<b>RESULTS AND DISCUSSION</b> .....	p. 11
<b>CONCLUSION</b> .....	p. 13
<b>ACKNOWLEDGEMENTS</b> .....	p. 14

## **INTRODUCTION**

The purpose of this project was to create a non-invasive, e-skin resistance sensor to measure both temperature and mechanical strain on whatever part of the body it was placed. The sensor was designed to conform to the anterior deltoid, but is able to conform to multiple different parts of the body with relative ease, and accuracy. The sensor for this project has undergone multiple iterations to reach the current design. The current design uses highly accurate laser cutting capabilities, which differ from initial iterations that used 3D printing, which introduced multiple issues with accuracy and repeatability of manufacture. The design of the device is a 4x2 array meant for mechanical strain sensing. Due to time constraints, the device was changed to become a temperature sensor, but future iterations could include mechanical strain capabilities. The device was designed using the 3D CAD software, Solidworks, but was converted to a vector file, as the laser cutter was able to cut the 2D image to the necessary depth required. Polydimethylsiloxane (PDMS) was chosen as the substrate material, and multi-walled carbon nanotubes (MWCNTs) were chosen as the conductive material due to their ease of accessibility, as both materials are very cheap and have been thoroughly studied. This report gives a detailed narrative of the design, fabrication, manufacture, and testing process, with insights for further work.

## **DESIGN THEORY AND WORKING PRINCIPLE**

Our project serves as an application of the cutting-edge work that has been done with transparent, elastic conductors, which are paving the way for the development of wearable devices with the ability to conform to the curved, irregular surfaces of the human body (Ray et al., 2019). As such, our design for a skin-like wearable temperature and potentially strain sensor

was developed via the careful threefold analysis of physiological, material, and engineering factors.

## **PHYSIOLOGICAL CONSIDERATIONS**

First and foremost, Miyamoto et al. (2017) signal the imperativeness to consider the biocompatibility of the chosen materials, as long-term psychological and physiological effects, can originate from improper electronic skin (E-skin) administration. Naturally, wearable electronics that interface with the skin should be minimally invasive, and the best results in this sense—measured in terms of the three principal factors of gas permeability, weight, and softness—are achieved with materials containing a porous, flexible structure. As such, irritation and discomfort can be reduced in long-term applications by introducing both stretchability and conformability to thin-film electronics, devices, and sensors. Planar substrates have always posed a challenge in enhancing these qualities (Miyamoto et al., 2017).

Further insight into desirable material properties can be found by evaluating the defining characteristics of human skin, namely self-reparative properties and mechanical compliance (Miyamoto et al., 2017). The latter allows skin to flex and stretch without incurring physical damage and exists as a result of its low mechanical modulus, a key element in the organ's ability to transmit physical properties to the receptors buried under the protective epidermis layer (Miyamoto et al., 2017). In turn, the resulting complex textures and eccentric natural motions cannot be accommodated by pure bending: the ability to flex only enables effective integration across "small regions of the body or those with simple, gradual curvature" (Ray et al., 2019). Here, it is critically important to study stretchability, as defined by "linear elastic responses to large strain deformations" (Ray et al., 2019).

## **MATERIAL CONSIDERATIONS**

Substrates have been a subject of great interest due to their desirable physical properties, extensive range of possible material compositions, and unique opportunity for highly efficient and economical manufacturing (Zardetto et al., 2011). Polydimethylsiloxane (PDMS) is currently the most widely applied thin-film substrate, with broad commercial availability and well-researched properties (Hammock et al., 2013). This popularity is largely a product of its numerous advantages, which include chemical inertness, stability over a wide range of temperatures, transparency, and variable mechanical properties (Hammock et al., 2013). E-skin applications rely heavily on PDMS's ability to define adhesive and non-adhesive regions through exposure to UV radiation, a specially important feature for bonding electronic materials to its surface (Hammock et al., 2013).

Carbon nanotube (CNT)-based active materials have likewise been remarked by preeminent researchers and engineers like Hammock et al. (2013) for their chemical stability and exceptional electronic and material properties. With proper alignment, a necessity for optimized performance, and near-ballistic transport has been achieved in defect-free tubes. From a fabrication standpoint, CNT networks are a superior choice, offering more uniform performance and better compatibility with conventional lithography and printing techniques. Moreover, stretchable conductors in both printed and photo-patterned versions have achieved excellent performance with the introduction of conductive materials like metallic spheres, flakes, and wires. The caliber of the conductor is principally determined by the relationship between this filler material and the matrix elastomer, as denoted in reports from Hammock et al. In general, large filler concentrations are typically associated with an enhanced elastic modulus and reduced strain at break. Nevertheless, anisotropic fillers have a low percolation threshold that generates

strong electrical properties at lower concentrations. As such, CNTs, which are both highly conductive and highly anisotropic, have been one of the most successful fillers. That being said, controlled aggregation into conductive pathways can additionally be employed to improve stretchable conductor design by reducing the required filler loading and enhancing conductivity (Hammock et al., 2013).

Large-scale reversible elasticity is perhaps the most desirable property for potential E-skin materials, and Hammock et al. reveal that it can be achieved using discontinuous structures that can distort while retaining electrical conductivity. Importantly, the discontinuous structures can be patterned at different length scales, yet still rely on similar mechanisms. Depositing a network of discontinuous, one-dimensional conductors limits the accumulation of stress and in turn, produces similar results to thin-film cracking. At a larger scale, deliberately patterning the discontinuous structures in convoluted, typically serpentine or horseshoe-shaped pathways can further reduce network strain. In this case, a primary concern is maintaining contact during stretching, but the long nanostructures in the network bridge conductive regions, thereby retaining electrical conductivity (Hammock et al., 2013).

## **ENGINEERING CONSIDERATIONS**

According to Ray et al., the development of stretchable electronics involves the application of synthetic materials. Bulk or laminar composites, a common synthetic material, are typically composed of active materials and dielectric elastomers such as silicones, polyurethanes, and copolymers. Internal charge transport occurs via two components: percolation pathways within a material and the collection of micro/nanostructures. The former supports the material's electronic functionality, while the latter defines its elastic mechanics and serves as a conductive filler embedded in an insulating elastomer matrix. In turn, the compositional ratio between these

two components determines the percolation threshold or the point at which the bulk material becomes conductive. By definition, the compositional ratio is inversely related to the aspect ratio, surface area, and dispersion of the conductive filler (Ray et al., 2019).

Ray et al. also illustrate how foundational work with composites in the context of stretchable electronics relies on conductive, multi-walled carbon nanotubes (MWCNTs). When used as the primary conductive constituent in laminar composites, MWCNTs can offer superior electrical properties to their bulk counterparts, largely due to both their ability to support thin-film geometries and their absence of an insulating component within the active layer. The most popular fabrication approach embeds thin films of carbon nanomaterials between elastomer layers. Typically, this is implemented by either the physical transfer or direct deposition of prefabricated films onto the elastomeric membranes. Mechanically, the system relies on the reversible, nonlinear buckling of the nanomaterials, which can be predictably modeled using Newtonian mechanics (Ray et al., 2019).

Most device designs involve compromising sensitivity to improve stretchability and vice-versa. Ray et al. observe that the use of multiple optimization strategies in a single device platform can mitigate the unique trade-offs associated with any particular method. In this sense, it is essential to consider a sensor's performance in terms of gauge factor (GF), as this metric is closely linked to changes in length and cross-sectional area for geometrically-induced changes in resistance. Yet, the most critical design criterion for any wearable electronic device ultimately lies in achieving the intimate, conformal contact necessary to support interface-dependent clinically relevant measurement modalities, such as electroencephalography (EEG), electromyography (EMG), electrocardiography (ECG), precision skin thermography, arterial tonometry, arterial tonometry, and vital sign monitoring (Ray et al., 2019).



## **PROJECT APPLICATIONS**

Drawing from the above physiological, material, and engineering considerations, the sensor is designed to capture the dynamic motions and temperature of the human body, with particular applications in clinical diagnostics (i.e., movement and neurological disorders) and athletic performance monitoring. In order to conform to size constraints and generate consistent clinically- and athletically-relevant measurements, the sensor is intended for placement on the anterior deltoid (shoulder). Resistive sensors in a 4x2 array are aligned to optimally measure uniaxial strain and temperature along the muscle fibers. For relative ease of manufacturability, the sensor employs an elastomeric substrate base with channels of conductors laminated to its surface. Taking into account relative commercial popularity and availability, polydimethylsiloxane (PDMS) was chosen as the substrate material, and multi-walled carbon nanotubes (MWCNTs) were chosen as the conductive material.

## **DESIGN AND FABRICATION**

### **MATERIALS PREPARATION**

As previously stated, the primary materials used to manufacture the temperature sensor are polydimethylsiloxane (PDMS) and multi-walled carbon nanotubes (MWCNTs). To create the PDMS solution, a 10:1 ratio of PDMS to curing agent (hexane) is mixed to promote the curing process. Once cured, the hexane is dissolved and only PDMS is left. To create an optimal layer, the area of the container was measured, and volume calculated. The PDMS mixture must be degassed in a pressurized environment to reduce imperfections in the material, and guarantee uniformity throughout the substance. Similarly, MWCNTs is mixed with a PDMS solution at a ratio of 10:1. The MWCNTs appear to be dustlike, and must be cured with a PDMS solution to conform and connect with the mold. The MWCNTs solution must also be degassed so as to

ensure full uniformity within the substance. Similar to the PDMS mold, the MWCNT solution must be cured on top of the mold for at least one day to guarantee full connection between parts.

## STRUCTURAL DESIGN

The structural design was developed based on previous resistive temperature sensor models, with a slightly adapted format designed to meet the needs of the particular use case. The layout was created on Solidworks, under a 4x2 strain array. The various measurements of the mold were first coded into a 3D modular form, providing for the thinnest possible mold, under the specific allowance of the 3D printer used (the printer had a tolerance of 1mm). Figure 1 on page 9 displays the manufacture sheet of the strain sensor, with specific measurements of the full device in millimeters.

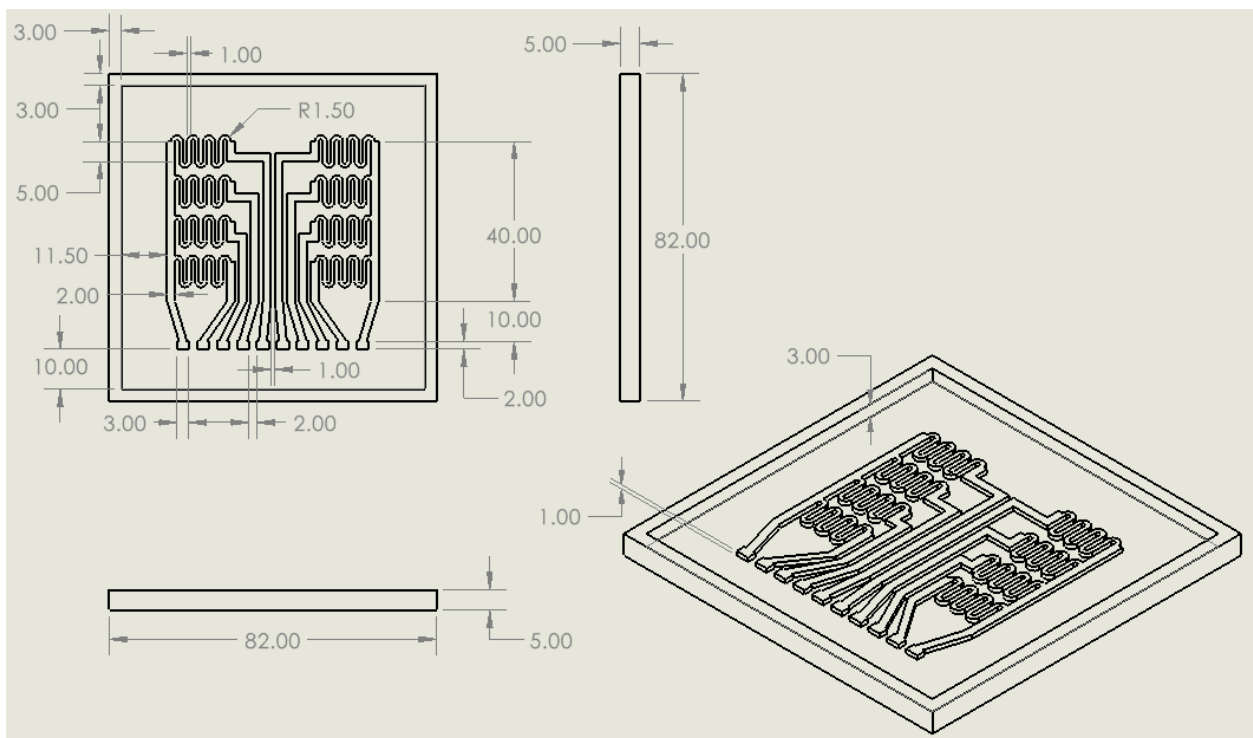


Figure 1: Sensor Mold Design with Measurements: The Solidworks part measurements and design sheet for the 3D sensor mold. (Ghatnekar et. al. 2022)

After various trials, under the specific specifications of an e-skin sensor, that must be as minimally invasive as possible, it was concluded that the mold procedure was not feasible. Due

to the higher tolerance of the machine when compared to our design, a K40 Laser Cutter was discovered as a solution to the tolerance problem. Using the same design as indicated above, a 2D vector drawing was rendered. This design as seen in Figure 2 on page 10 below, was uploaded to the K40 Laser Cutter so as to implement a more precise cut directly into a layer of PDMS to minimize room for error.

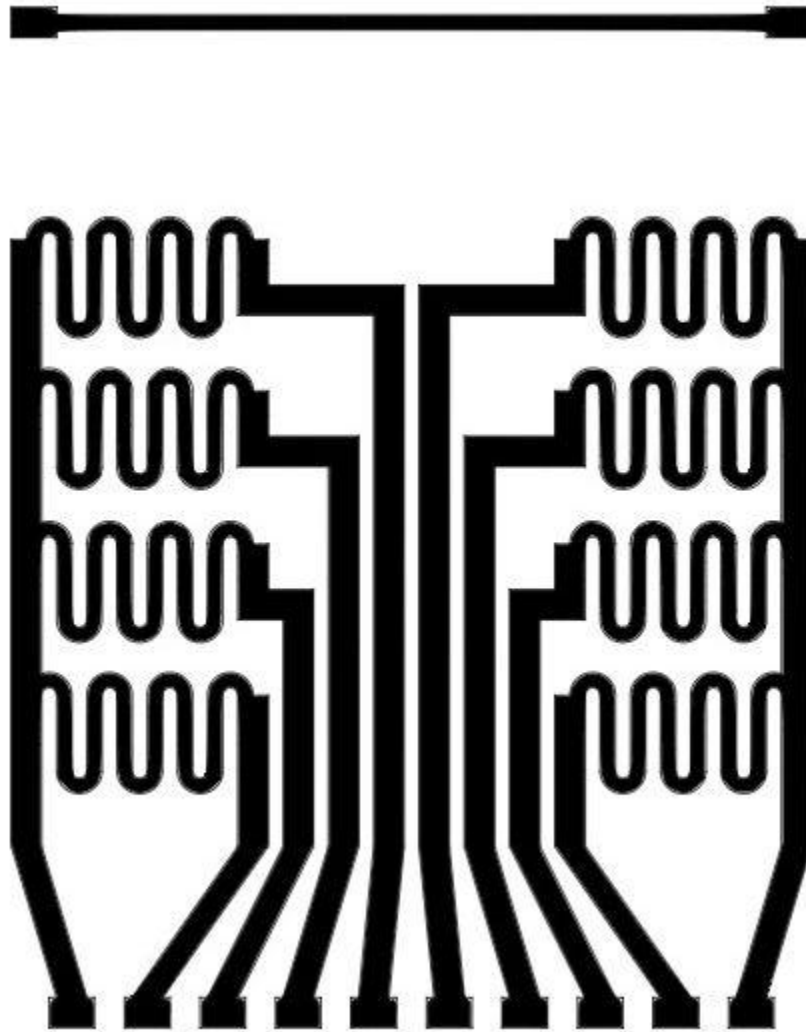


Figure 2: 2D Vector Sensor Design: The vector image of the design, used in laser cutting with the K40 Laser Cutter. (Ghatnekar et. al. 2022)

## FABRICATION

Fabrication of the wearable was a multistep process. First, the area of the petri dish where the sensor was made was measured. The dish had a radius of 7 mm, and therefore an area of about 153.9 mm<sup>2</sup>. The volume of the petri dish was then measured, as the PDMS solution needed to be 2 mm thick, so that the MWCNT channels could be 1 mm thick. The PDMS solution, at a 10:1 ratio, was measured using a scale and a mixing capsule. Under the assumption that the density of PDMS is 1 kg/m<sup>3</sup>, the PDMS was measured to 31 g, and the hexane curing agent was measured to 3.1 g. The mixture was, then, mixed and degassed until there were no visible bubbles, or impurities, within the solution. Finally, the petri dish was sprayed with a desticking spray, for ease of removal of the device once manufactured, and the device was cured overnight.

Next, the K40 Whisper software was used to cut into the PDMS solution to create a mold for the MWCNT mixture to be laid. The laser was operated at a Raster speed of 40 mm/s, operating at 9% power to engrave the cured substance as fast as possible, while not sacrificing precision, and optimizing safety. The process of laser cutting can be seen in Figure 3 below.

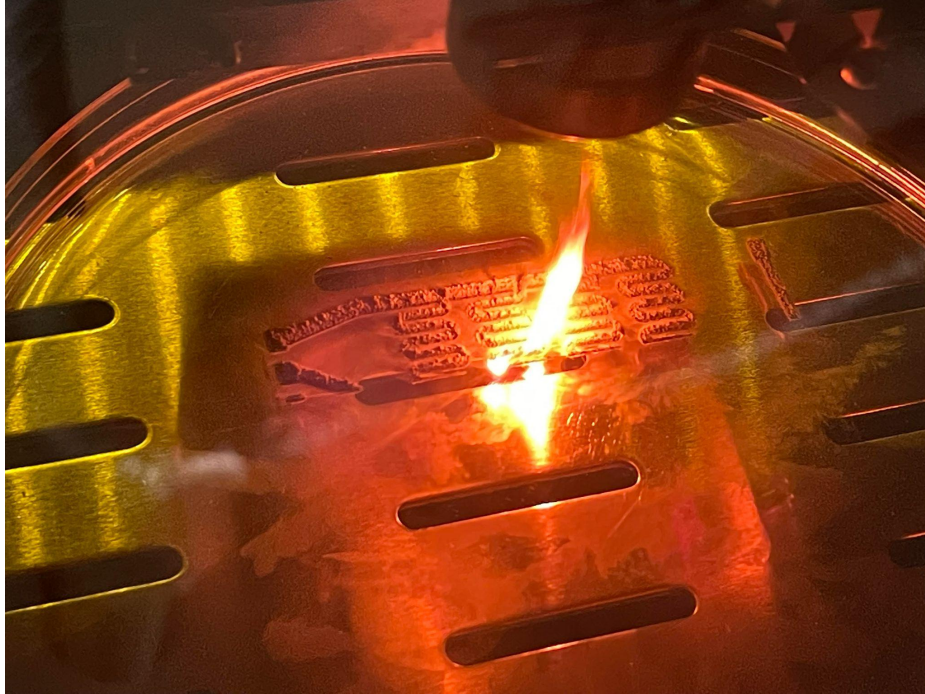


Figure 3: Laser Cutting of Mold: Laser cutting process of the mold, showing the intensity and precision of the cutting process. (Ghatnekar et. al. 2022)

The laser left certain byproduct behind that was not conductive, and therefore was necessary to clean off. Using an ethanol solution, as well as an air jet, the cut PDMS was washed off, so as to provide a clean surface for MWCNT solution application.

Similar to the PDMS solution process, the MWCNTs were also mixed at a 10:1 ratio. It was necessary to mix this solution at a high ratio, as the resistivity of the substance increases with higher MWCNT concentrations. The MWCNTs were mixed with the PDMS and hexane, at the same ratio as indicated above, and the solution was mixed in a UV bath to ensure full MWCNT matriculation and uniformity within the substance. After a minimum of 3 hours, the solution was removed and coated on the channels of the device. Next, the device is placed in a pressure chamber to degas again, The tedious process of coating takes multiple cycles. The first cycle completes an initial coating, but the MWCNT mixture shrinks after curing due to the evaporation of hexane from the solution during the curing stage. After multiple cycles of

MWCNT coating, degassing, and curing the device looked uniform with a uniform top layer. Wires were then added at the pads of the device so that mechanical testing may be completed. Finally, the device was removed from the petri dish, and the petri dish was sprayed and cleaned again. A PDMS mixture at a 10:1 ratio was created, though only 15 g of PDMS solution are created, degassed, and poured into the petri dish. The device was layed face down into the petri dish and placed on top of the thin PDMS layer to coat and seal the device. Once cured, the device is removed, and excess PDMS is removed, finalizing the fabrication process.

## RESULTS AND DISCUSSION

To test the accuracy of the device measurement, a temperature test was performed. Using a test strip from the manufactured design, as shown in Figure 4, the necessary calculations for the resistance vs. temperature relationship were measured.



Figure 4: Testing Sensor Strip: To test the mechanical properties of the device, a smaller strip was developed using the same process that was indicative of how the full device would work. (Ghatnekar et. al. 2022)

First, the resistance of the device was measured at room temperature (25 °C). To measure the resistance, a Fluke 101 600V CAT III Multimeter was used, measuring the resistance of the sensor in k $\Omega$ . Next, the device was placed on a Thermo Scientific hot plate, and the temperature of the device was raised in increments of 5 °C until the temperature reached 45 °C. The temperatures were chosen, as they are the closest related to the range of human skin temperature. At each temperature, the device was allowed to rest for approximately 3 minutes to ensure full device uniformity in temperature. Subsequently, 3 different measurements were recorded at each

temperature in 30 second intervals. The method for recording is diagramed in the schematic in Figure 5 below.

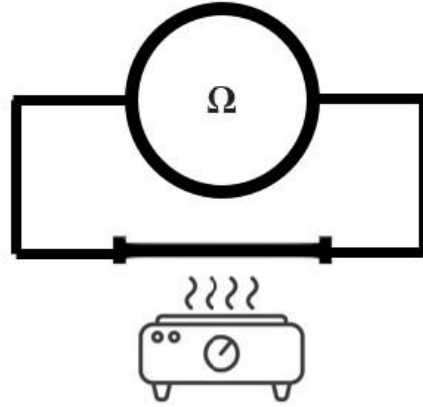


Figure 5: Schematic for Electrical Response to Temperature Testing: The method for device temperature testing, using a hot-plate, with the sensor connected to an ohmmeter, measuring the resistance of the device in  $k\Omega$ . (Ghatnekar et. al. 2022)

The process was repeated in two different samples of varying thickness, one that was 3.5mm thick, and one that was 4mm thick. Once completed, the response to temperature was analyzed under the differing temperatures to analyze if the coefficient of temperature was the same for both samples, therefore confirming if the MWCNT mixture would be usable in future measurements and iterations of the study. Using the equation,  $\frac{\Delta R}{R_0} = \alpha T + 1$ , where  $\Delta R$  is the change in resistance of the sensor at varying temperatures,  $R_0$  is the initial measured resistance of the sensor at room temperature (25 °C),  $\alpha$  is the coefficient of temperature, and T is the measured temperature in °C. The recorded data for each sensor can be found in Appendix A.

The correct resistance ratio,  $\frac{\Delta R}{R_0}$ , the temperature ratio was assumed to be the same as that of a uniform metal, meaning a purely linear measurement. As seen in Figures 6, both the 3.5 mm and 4 mm molds had a relatively linear distribution.

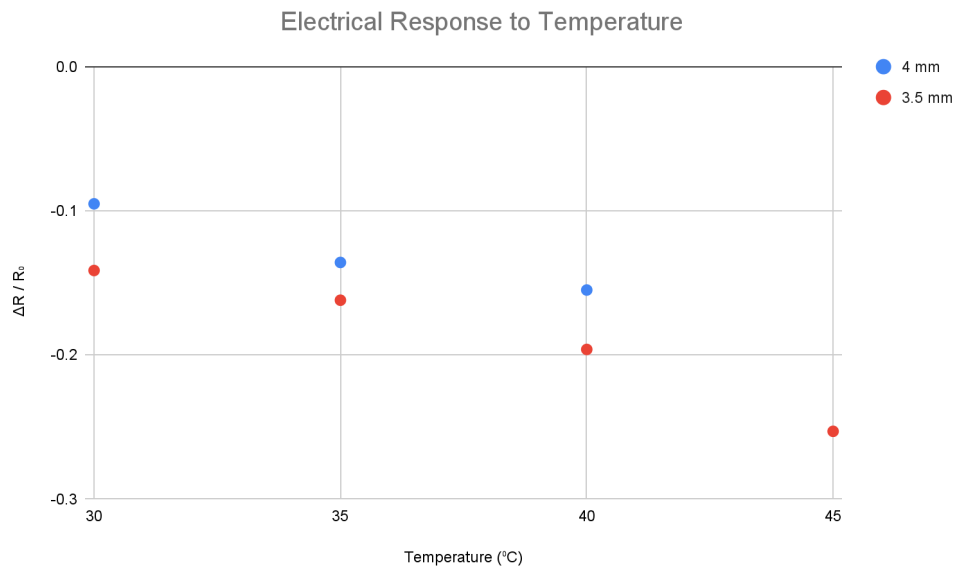


Figure 6: Electrical Response to Temperature Graph: The graph of the resistance ratio to temperature relationship for both mold thicknesses, to find the coefficient of temperature. (Ghatnekar et. al. 2022)

The measured  $\alpha$  for the 3.5 mm mold was  $-0.0326 \text{ C}^{-1}$ , while the 4 mm mold had a measurement of  $-0.0322 \text{ C}^{-1}$ . While both were not exactly the same, they differed by about 1%, which is fairly accurate. It is worth noting that the data for the 4 mm mold is lacking a data point at 45  $^{\circ}\text{C}$ . It is unknown as to why the device failed to record a resistance measurement at this temperature, but can be hypothesized that the wire connection to the MWCNT channel within the sensor failed, and the sensor was broken, rendered useless. Interestingly, the measurements for resistance were all about 4% lower for the 3.5 mm compared to the 4 mm mold. This may be attributed to the random nature of the MWCNT connections and the channel, as well as the greater relative thickness of the MWCNT channels compared to the rest of the sensor thickness.

## CONCLUSION

Due to time and monetary constraints, the sensor was not able to be tested on human subjects. Similarly, the device was unable to undergo mechanical strain testing, so as to be applied in a sporting/biomechanical environment. Also, for future applications of this project, the



wire materials must be further analyzed, and a new method for wire implementation must be included. With the current results, further analysis of the MWCNT and temperature relationship may be conducted to analyze the relationship between the resistance ratio and temperature within this material. If possible, an exact value for the temperature coefficient would make the creation of more sensors using this method easily repeatable, scalable and feasible. While the sensor is still not able to provide use on human subjects, further research into the sensor, and further design and fabrication with the laser sensor could create a viable, exact, and precise sensor for human testing.

### **ACKNOWLEDGMENTS**

Thank you to the Department of Mechanical and Aerospace Engineering at the University of Virginia for their sponsorship of the group. All materials, as well as the room and equipment was provided by this department.

Thank you to Professor Baoxing Xu of the Department of Mechanical Engineering at the University of Virginia for the Advisement during this project. Professor Xu taught the team about all sensors, and provided the team with key insight into the design, manufacture, fabrication, and testing of the sensors.

Thank you to Yimin Gao, a Graduate Mechanical Engineering student, for his time and aid during the development and testing of the project.

## REFERENCES

- Hammock, M. L., Chortos, A., Tee, B. C.-K., Tok, J. B.-H., & Bao, Z. (2013). 25th anniversary article: The evolution of electronic skin (E-skin): A brief history, design considerations, and recent progress. *Advanced Materials*, *25*(42), 5997-6038.  
<https://doi.org/10.1002/adma.201302240>
- Miyamoto, A., Lee, S., Florence Cooray, N., Lee, S., Mori, M., Matsuhisa, N., Jin, H., Yoda, L., Yokota, T., Itoh, A., Sekino, M., Kawasaki, H., Ebihara, T., Amagai, M., & Someya, T. (2017). Inflammation-free, gas-permeable, lightweight, stretchable on-skin electronics with nanomeshes. *Nature Nanotechnology*, *12*, 907-913.  
<https://doi.org/10.1038/nnano.2017.125>
- Ray, T. R., Choi, J., Bandodkar, A. J., Krishnan, S., Gutruf, P., Ghaffari, R., & Rogers, J. A. (2019). Bio-integrated wearable systems: A comprehensive review. *Chemical Reviews*, *119*(8), 5461-5533. <https://pubs.acs.org/doi/10.1021/acs.chemrev.8b00573>
- Zardetto, V., Brown, T. M., Andrea, R., & Di Carlo, A. (2011). Substrates for flexible electronics: A practical investigation on the electrical, film flexibility, optical, temperature, and solvent resistance properties. *Journal of Polymer Science Part B: Polymer Physics*, *49*(9), 638-648. <https://onlinelibrary.wiley.com/doi/10.1002/polb.22227>